Dynamic Modeling and Simulation of a Flexible Two-Wheeled Balancing Robot

Xiaogang Ruan, Xinyuan Li*, and Xuetao Xing

College of Electronic Information and Control Science, Beijing University of Technology, Beijing 100124, China
adrxg@bjut.edu.cn, {li_xinyuan,tonyxing722}@emails.bjut.edu.cn

Abstract. This paper focuses on deriving the dynamic model of a novel flexible mobile robot, which has elastic joint, so that the robot is able to be simulated with a computer and analyzed dynamically. First, the dynamic equations are derived from Routh formulation with the nonholonomic constraints of the robot, and then the nonholonomic constraint forces are removed so that the dynamic equations are transformed to an input-affine form at last. Three illustrative simulation results are given which show that the dynamic model presented in this paper is reasonable.

Keywords: two-wheeled balancing robot, elastic joint, dynamic modeling.

1 Introduction

Two-wheeled balancing robot (TWBR), whose wheels are parallel and mass center is above the wheels' axis, is a kind of highly maneuverable mobile robot. It is a typical object in control science area to practise kinds of control policy [1, 2, 3].

Basing on many famous TWBRs [1, 10, 11], some advanced mobile manipulators [4, 5, 12] are developed. Besides, PT vehicle [11] from Segway Corp. is the most successful merchant application of TWBR. These existing TWBRs can be approximate to a system of rigid bodies, but the flexibility must be considered when the size of the robots get bigger and mass get smaller. Otherwise, the driver of PT can be considered as a flexible load, so the vehicle is a rigid-flexible system actually. Hence, it is valuable to build a flexible TWBR and derive its dynamic model for analyzing its flexible feature and improving control system's performance.

"Flexible robot" basically limits to manipulators so far, there is no report about flexible body TWBR. The elastic beam of flexible manipulator is inadequate to build a TWBR because of its load-insufficiency. The structure of inverted pendulum with elastic joint in [6, 7] is simple and durable, and is consistent with the idea of the finite segment approach [8] for the dynamics of flexible-multibody system, so it is suitable to build a TWBR. But there are two springs in [6], which is redundant and parameter-coupling; and the elastic joint in [7] is just imaginary for mathematical modeling.

The dynamic model of those conventional TWBRs [1, 2, 9] can not be use to describe a flexible TWBR. Otherwise, because the motors' location of TWBR is different from those inverted pendulums and TWBR has yawing degree [2], the dynamic model of [6, 7] is not proper for a flexible TWBR.

* Corresponding author.

C. Xiong et al. (Eds.): ICIRA 2008, Part I, LNAI 5314, pp. 1011–1020, 2008.

Hence, this paper describes a flexible body TWBR named "Hominid 1", which has an elastic passive rotation-joint as its waist.

Then, we focus on deriving the dynamic model of the robot using Routh formulation of the nonholonomic system so that the robot is able to be simulated and analyzed dynamically.

Finally, three illustrative simulations are given to verify the model qualitatively. The first one tests the flexibility of the elastic joint of the robot. The second one is the robot falls from the upright position free. In the third one, two different torques are given to the wheels to test the yaw of the robot. All varying of the robot in above three situations is consistent to real physical phenomenon, which indicates that the dynamic model presented in this paper is reasonable.

2 TWBR with Elastic Joint

The Hominid 1 is similar to other TWBRs except its elastic "waist". Fig.1 shows the construction of the waist. It is a rotation-joint connecting the truck to the chassis, and there is a spring between the around the joint, which looks like a sleeve. Thus, the truck can turn around on the axis of the joint; meanwhile, the rotation is constrained by the elasticity of the spring. The robot can represent limited flexibility.

The waist is simple, low-cost and replaceable, so it is very suitable to build a flexible TWBR.

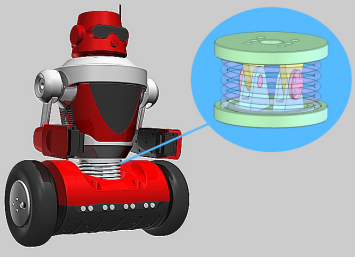

Fig. 1. "Hominid 1" and its "waist"

3 Dynamic Modeling

This section derives the dynamic model of Hominid 1 using Lagrangrian approach.

First of all, the robot is simplified to an abstract model (Fig.2). Point B represent the joint, P0B and AB is symmetric-mass rigid body, named body1 and body2. The mass of the spring and the inertia of the motor rotor can be ignored because they are far smaller than other parts.

Define a fixed coordinate {OXYZ}. The adherent coordinates $\{OXYZ\}_{b1}$ and $\{OXYZ\}_{b2}$ parallel to {OXYZ}, and their origins are fixed to centroid of body1 and body2, respectively. The robot moves in the plane XOY without air resistance, slip and constriction (except the constriction between wheels and ground). The physical parameters are defined as Tab.1.

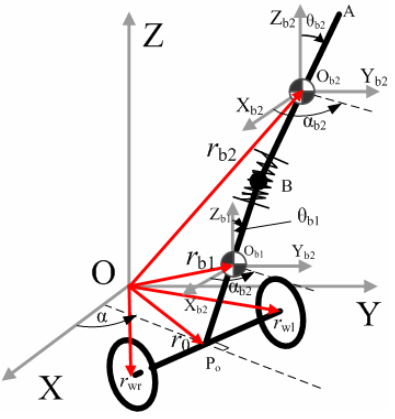

Fig. 2. The simplified model of Hominid 1

Table 1. The physical parameters of Hominid 1

Parameter	Symbol	Value
Mass of the body1,body2	M_{b_1,b_2}	10kg,10kg
Mass of the wheel	M_w	1.5kg
Height of the body1,body2	H_{b_1,b_2}	0.4m,0.25m
Length of the chassis	L_{b_1,b_2}	0.4m
Radius of the wheel	R_w	0.15m
Bending Stiffness constant of the spring	k	25N/rad
Bending Damp constant of the spring rotation	d	$1Ns^2/rad^2$
Acceleration of gravity	g	$9.8m/s^2$
Roll friction force between the wheel and ground	F	5N

3.1 Kinetic Energy and Potential Energy

First, the vector of every part's centroid is given as coordinate matrix in {OXYZ}.

$$\underline{\mathbf{r}}_{\mathbf{0}} = [x \; y \; z]^{\mathrm{T}}. \tag{1}$$

$$\underline{\mathbf{r}}_{\mathbf{b_1}} = \left[x + \frac{H_{b_1}}{2}\mathrm{s}\theta_{b_1}\mathrm{c}\alpha \quad y + \frac{H_{b_1}}{2}\mathrm{s}\theta_{b_1}\mathrm{s}\alpha \quad z + \frac{H_{b_1}}{2}\mathrm{c}\theta_{b_1} \right]^{\mathrm{T}}. \tag{2}$$

$$\underline{\mathbf{r}}_{\mathbf{b_2}} = \begin{pmatrix} x + H_{b_1}\,\mathrm{s}\theta_{b_1}\,\mathrm{c}\alpha + \dfrac{H_{b_2}}{2}\mathrm{s}\theta_{b_2}\mathrm{c}\alpha \\ y + H_{b_1}\,\mathrm{s}\theta_{b_1}\,\mathrm{s}\alpha + \dfrac{H_{b_2}}{2}\mathrm{s}\theta_{b_2}\mathrm{s}\alpha \\ z + H_{b_1}\mathrm{c}\theta_{b_1} + \dfrac{H_{b_2}}{2}\mathrm{c}\theta_{b_2} \end{pmatrix}. \tag{3}$$

$$\underline{\mathbf{r}}_{\mathbf{w}_l} = \left[x - \frac{1}{2} L_{b_1} \mathrm{s}\alpha \quad y + \frac{1}{2} L_{b_1} \mathrm{c}\alpha \quad 0 \right]^{\mathrm{T}}. \tag{4}$$

$$\underline{\mathbf{r}}_{\mathbf{w}_r} = \left[x + \frac{1}{2} L_{b_1} \mathrm{s}\alpha \quad y - \frac{1}{2} L_{b_1} \mathrm{c}\alpha \quad 0 \right]^{\mathrm{T}}. \tag{5}$$

"s" means "sine", and "c" means "cosine" in this paper.

The second step is describing the angular velocity vectors of all parts with coordinate matrices and obtaining the inertia matrices.

The matrices have identical form, because all parts rotate with same way in their adherent coordinate, which can be decompose to turning θ around Y-axis and then turning α around Z-axis.

The angular velocity vector's coordinate matrix is:

$$\underline{\boldsymbol{\omega}} = [\dot{\alpha} \mathrm{s}\theta \quad \dot{\theta} \quad \dot{\alpha} \mathrm{c}\theta]^T. \tag{6}$$

All inertia matrices have the same form as:

$$\underline{\mathbf{J}} = \begin{pmatrix} J_{xx} & 0 & 0 \\ 0 & J_{yy} & 0 \\ 0 & 0 & J_{zz} \end{pmatrix}. \tag{7}$$

The kinetic energy of single body is:

$$T = T^T + T^R = \frac{1}{2} \dot{\underline{\mathbf{r}}}^{\mathrm{T}} M \dot{\underline{\mathbf{r}}} + \frac{1}{2} \underline{\boldsymbol{\omega}}^{\mathrm{T}} \underline{\mathbf{J}} \underline{\boldsymbol{\omega}}. \tag{8}$$

The kinetic energy of system is:

$$T = T_{w_l}^T + T_{w_l}^R + T_{w_r}^T + T_{w_r}^R + T_{b_1}^T + T_{b_1}^R + T_{b_2}^T + T_{b_2}^R \ . \tag{9}$$

The potential energy of the system includes the gravitational potential energy is:

$$U^G = U_{b_1}^G + U_{b_2}^G = \frac{M_{b_1} g H_{b_1}}{2} \mathrm{c}\theta_{b_1} + M_{b_2} g (H_{b_1} \mathrm{c}\theta_{b_1} + \frac{H_{b_2}}{2} \mathrm{c}\theta_{b_2}) \ , \tag{10}$$

and the elastic potential energy is:

$$U^E = \frac{k}{2} (\theta_{b_2} - \theta_{b_1})^2. \tag{11}$$

3.2 The Dynamic Equations

The generalized coordinates of the system are initially taken as:

$$\mathbf{q} = \left[x \quad y \quad \alpha \quad \theta_{b_1} \quad \theta_{b_2} \quad \varphi_l \quad \varphi_r \right]^{\mathbf{T}}. \tag{12}$$

The robot has nonholonomic constraints, so the dynamic equations can be derived using Routh formulation:

$$\frac{d}{dt}(\frac{\partial L}{\partial \dot{\mathbf{q}}})-\frac{\partial L}{\partial \mathbf{q}}+\frac{\partial D}{\partial \dot{\mathbf{q}}}=\mathbf{E}(\mathbf{q})\mathbf{u}+\mathbf{A}^{\mathrm{T}}(\mathbf{q})\boldsymbol{\lambda}\,. \tag{13}$$

where

$$L=T-U^{G}-U^{E} \tag{14}$$

is the Lagrangian function;

$$D=\frac{c}{2}(\dot{\theta}_{b_2}-\dot{\theta}_{b_1})^2+FR_w(\dot{\varphi}_l+\dot{\varphi}_r) \tag{15}$$

is the dissipation energy, where F is the roll friction force;

$$\mathbf{E}(\mathbf{q})\mathbf{u}=\begin{pmatrix}0&0&0&-1&0&1&0\\0&0&0&-1&0&0&1\end{pmatrix}^{\mathbf{T}}\begin{pmatrix}\tau_l\\\tau_r\end{pmatrix} \tag{16}$$

is the generalized force, where $\mathbf{u}$ is the vector of motor output torques; $\boldsymbol{\lambda}$ is the constraint-forces vector, and

$$\mathbf{A}(\mathbf{q})=\begin{pmatrix}-\mathrm{s}\alpha&\mathrm{c}\alpha&0&0&0&0&0\\\mathrm{c}\alpha&\mathrm{s}\alpha&L_{b_1}/2&0&0&-R_w&0\\\mathrm{c}\alpha&\mathrm{s}\alpha&-L_{b_1}/2&0&0&0&-R_w\end{pmatrix} \tag{17}$$

is a matrix derived from the nonholonomic constraints:

$$\mathbf{A}(\mathbf{q})^{\mathrm{T}}\dot{\mathbf{q}}=0\,. \tag{18}$$

Equation (13) can be written as:

$$\mathbf{M}(\mathbf{q})\ddot{\mathbf{q}}+\mathbf{V}(\mathbf{q},\dot{\mathbf{q}})=\mathbf{E}(\mathbf{q})\mathbf{u}+\mathbf{A}^{\mathrm{T}}(\mathbf{q})\boldsymbol{\lambda}\,. \tag{19}$$

$\boldsymbol{\lambda}$ in (19) can be eliminated by multiplying $\mathbf{S}(\mathbf{q})$ to both sides of (19).

$$\mathbf{S}(\mathbf{q})=\begin{pmatrix}c\alpha&s\alpha&0&0&0&1/R_w&1/R_w\\0&0&1&0&0&L_{b_1}/2R_w&-L_{b_1}/2R_w\\0&0&0&1&0&0&0\\0&0&0&0&1&0&0\end{pmatrix}. \tag{20}$$

Otherwise, there is a transform equation:

$$\dot{\mathbf{q}}=\mathbf{S}^{\mathbf{T}}(\mathbf{q})\dot{\mathbf{q}}_r\,, \tag{21}$$

where

$$\dot{\mathbf{q}}_r=\begin{bmatrix}\dot{r}_0&\dot{\alpha}&\dot{\theta}_{b_1}&\dot{\theta}_{b_2}\end{bmatrix}^{\mathrm{T}}. \tag{22}$$

Finally, define state vector as:

$$\mathbf{X} = [\mathbf{q}_r \quad \dot{\mathbf{q}}_r]^{\mathrm{T}}, \tag{23}$$

Thus, the input-affine form of the robot's dynamic equations is given by:

$$\mathrm{M}(\mathbf{X})\dot{\mathbf{X}} = \mathrm{F}(\mathbf{X}) + \mathrm{G}(\mathbf{X})\mathbf{u}, \tag{24}$$

where

$$\mathrm{M}(\mathbf{X}) = \begin{pmatrix} \mathbf{I}_{4\times4} & \mathbf{0}_{4\times4} \\ \mathbf{0}_{4\times4} & \mathbf{m}(\mathbf{q})_{4\times4} \end{pmatrix}_{8\times8}, \ \mathrm{F}(\mathbf{X}) = \begin{pmatrix} \mathbf{q}_r \\ \mathbf{f}(\mathbf{q},\dot{\mathbf{q}}) \end{pmatrix}_{8\times1}, \mathrm{G}(\mathbf{X}) = \begin{pmatrix} \mathbf{0}_{4\times2} \\ \mathbf{SE}(\mathbf{q}) \end{pmatrix}_{8\times2}. \tag{25}$$

The detail expressions of (26) are provided in the appendix.

4 Simulation

Basing on L-K numerical integration method, we solve (25) to simulate three movements of the robot, of which the results in the real world is known, so comparing the simulation results with the real results can verify the dynamic model of the robot qualitatively. The parameter values for simulation are in Table 1.

In the first simulation, the chassis and wheels of the robot are fixed in the upright position all the time, and the truck's rotational angular θ_{b_1} is initialized to 0.2 radian. Fig.3 illustrates the angular variation of the robot's body, in which the vibrational convergence of θ_{b_1} is obviously consistent to the truth. This simulation shows the flexibility of the robot's body clearly.

In the second simulation, the truck is given an initial angular (0.5 radian) to the upright position in order to make the robot fall down free. Fig.4 records the angular

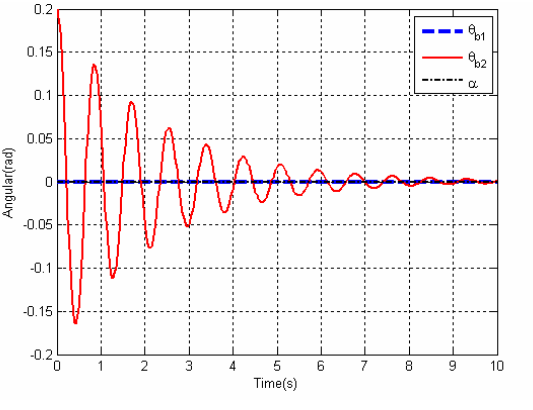

Fig. 3. The flexibility of the robot

variation of the robot's body. Notes that there is no constraint to stop the falling when the robot's body crashes the ground (θ_{b_1} or $\theta_{b_2} = \pi/2$), so θ_{b_1} and θ_{b_2} wave around and converge at π , which is the minimizing energy point of the system, and they vary relatively but the waving range of θ_{b_2} is larger because of the effect of the elastic joint. Besides, the angular α is zero always due to no torque for Z-axis. These results are acceptable to verify the dynamic model is correct.

In the third simulation, the robot is imagined in plumb position without constraint force, and then its wheels are given two different torques ($M = [0 \quad 1]^T$). Fig. 5 shows that the variation of the jaw angular is increasing all the time, but it is nonlinear at the beginning due to the body's swing. This result is consistent to the jaw of the robot.

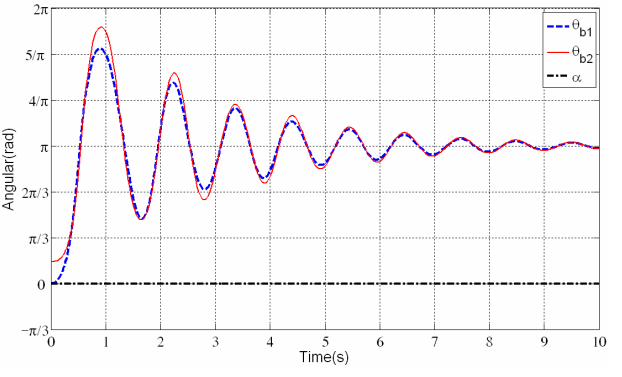

Fig. 4. The angular variation when the robot falls down free

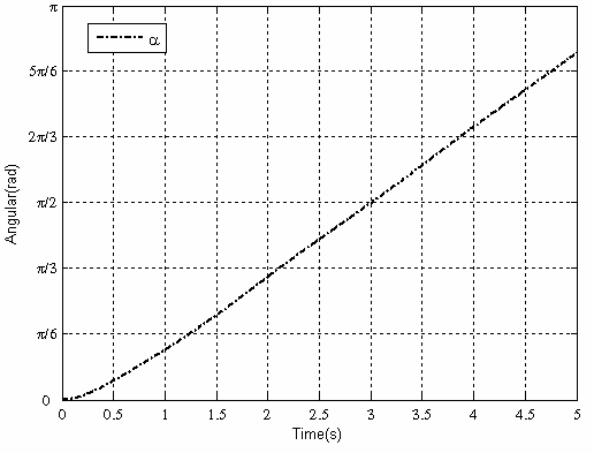

Fig. 5. The angular variation when the robot jaws

5 Conclusion

In this paper, we describe a new type flexible TWBR "Hominid 1", which has an elastic joint as its waist. The waist is simple, low-cost and replaceable, so it is a very suitable flexible module to construct TWBR.

Then, we focus on deriving the dynamic model of the robot so that the robot is able to be simulated and analyzed. The Routh formulation is used to derive the dynamic equations of the nonholonomic robot system. After eliminating the nonholonomic constraint forces, the input- affine equations are derived as the dynamic model finally.

Three illustrative simulations are given to verify the model qualitatively. The results of three simulations indicate that the dynamic model of the robot is reasonable, and the model can be useful to simulate or analyze the feature of the flexible TWBR.

Acknowledgement

This work is supported by NSFC (60774077), 863 program of China (2007AA04Z226), BMEC(KZ200810005002) and BMSF.

References

1. Grasser, F., D'Arrigo, A., Colombi, S.: JOE: A Mobile, Inverted Pendulum. IEEE T. Ind. Electron. 49, 107–114 (2002)
2. Pathak, K., Franch, J., Agrawal, K.: Velocity and Position Control of a Wheeled Inverted Pendulum by Partial Feedback Linearization. IEEE T. Robot. 21, 505–513 (2005)
3. Ren, T.J., Chen, T.C., Chen, C.J.: Motion control for a two-wheeled vehicle using a self-tuning PID controller. Control. Eng. Pract. 13, 366–375 (2008)
4. Thibodeau, B.J., Deegan, P., Grupen, R.: Static analysis of contact forces with a mobile manipulator. In: 2006 IEEE International Conference on Robotics and Automation, pp. 4007–4012. IEEE Press, Orlando (2006)
5. Ambrose, R.O., et al.: Mobile manipulation using NASA's Robonaut. In: 2004 IEEE International Conference on Robotics and Automation, pp. 2104–2109. IEEE Press, New Orleans (2004)
6. Kawaji, S., Kanazawa, K.: Control of Double Inverted Pendulum with Elastic Joint. In: 1991 IEEE Intelligent Robot and System, pp. 946–951. IEEE Press, Osaka (1991)
7. Galan, J., Fraser, W.B., Acheson, D.J., Champneys, A.R.: The parametrically excited upside-down rod: an elastic jointed pendulum model. J. Sound. Vib. 280, 359–377 (2005)
8. Connelly, J.D., Huston, R.L.: The dynamics of flexible multibody system: a finite segment approach -I. theoretical aspects. Comput. Struct. 50, 255–258 (1994)
9. Salerno, A., Angeles, J.: On the nonlinear controllability of a quasiholonomic mobile robot. In: 2003 IEEE International Conference on Robotics and Automation, pp. 3379–3384. IEEE Press, Taiwan (2003)
10. nbot, `http://www.geology.smu.edu/~dpa-www/robo/nbot/`
11. PT&RMP, `http://www.segway.com`
12. Partner robot, `http://www.toyota.co.jp/en/special/robot/`

Appendix

$$\mathbf{m(q)} = \mathbf{SM(q)S}^{\mathrm{T}} = \begin{pmatrix} m_{11} & 0 & m_{13} & m_{14} \\ 0 & m_{22} & 0 & 0 \\ m_{13} & 0 & m_{33} & m_{34} \\ m_{14} & 0 & m_{34} & m_{44} \end{pmatrix}. \tag{26}$$

$$m_{11} = M_{b_1} + M_{b_2} + 2M_w + 2J_{wyy} / R_w{}^2 \,, m_{13} \frac{M_{b_1} H_{b_1} + 2M_{b_2} H_{b_1}}{4} \mathrm{c}\theta_{\mathrm{b}_1} \,,$$

$$m_{14} = \frac{M_{b_2} H_{b_2}}{4} \mathrm{c}\theta_{\mathrm{b}_2} \,,\ m_{33} = \frac{M_{b_1} H_{b_1}{}^2}{4} + J_{b_1 yy} + M_{b_2} H_{b_1}{}^2 \,,$$

$$m_{22} = (M_w L_{b_1}{}^2 + J_{wxx} + J_{b_1 zz} + J_{b_2 zz} + \frac{J_{wyy} L_{b_1}{}^2}{2R_w{}^2}) + (\frac{M_{b_2} H_{b_2}{}^2}{4} + J_{b_2 xx} - J_{b_2 zz}) \sin^2 \theta_{\mathrm{b}_2}$$
$$+ (\frac{M_{b_1} H_{b_1}{}^2}{4} + J_{b_1 xx} + M_{b_2} H_{b_1}{}^2 - J_{b_1 zz}) \sin^2 \theta_{\mathrm{b}_1} + \frac{M_{b_2} H_{b_1} H_{b_2}}{2} \sin\theta_{b_1} \sin\theta_{\mathrm{b}_2}$$

$$m_{34} = \frac{M_{b_2} H_{b_1} H_{b_2}}{4} \mathrm{c}(\theta_{b_2} - \theta_{\mathrm{b}_1}) \,,\ m_{44} = \frac{M_{b_2} H_{b_2}{}^2 + 4J_{b_2 yy}}{4} \,. \tag{27}$$

$$\mathbf{f(q, \dot{q}_r)} = -\mathbf{S}[\mathbf{M(q)}\dot{\mathbf{S}}^{\mathrm{T}}\dot{\mathbf{q}}_r + \mathbf{V(q, \dot{q})}] = \begin{pmatrix} f_1 & f_2 & f_3 & f_4 \end{pmatrix}^{\mathrm{T}}, \tag{28}$$

$$f_1 = \frac{M_{b_1} H_{b_1} + 2M_{b_2} H_{b_1}}{4} (\dot{\theta}_{\mathrm{b}_1}{}^2 \mathrm{s}\theta_{\mathrm{b}_1} + \dot{\alpha}^2 \mathrm{s}\theta_{\mathrm{b}_1}) + \frac{M_{b_2} H_{b_2}}{4} (\dot{\theta}_{\mathrm{b}_2}{}^2 \mathrm{s}\theta_{\mathrm{b}_2} + \dot{\alpha}^2 \mathrm{s}\theta_{\mathrm{b}_2}) - \frac{2F}{R_w} \,,$$

$$f_2 = [(-\frac{M_{b_1} + 4M_{b_2}}{4} H_{b_1}{}^2 - J_{b_1 xx} + J_{b_1 zz}) \dot{\theta}_{\mathrm{b}_1} \sin 2\theta_{\mathrm{b}_1} - \frac{M_{b_2} H_{b_1} H_{b_2}}{2} \dot{\theta}_{\mathrm{b}_1} \cos\theta_{b_1} \sin\theta_{\mathrm{b}_2}$$
$$- (\frac{M_{b_2} H_{b_2}{}^2}{4} + J_{b_2 xx} - J_{b_2 zz}) \dot{\theta}_{\mathrm{b}_2} \sin 2\theta_{\mathrm{b}_2} - \frac{M_{b_2} H_{b_1} H_{b_2}}{2} \dot{\theta}_{\mathrm{b}_2} \sin\theta_{b_1} \cos\theta_{\mathrm{b}_2} \quad ,$$
$$- \dot{\alpha} (\frac{M_{b_1} H_{b_1} + 2M_{b_2} H_{b_1}}{4} \mathrm{s}\theta_{\mathrm{b}_1} + \frac{M_{b_2} H_{b_2}}{4} \mathrm{s}\theta_{\mathrm{b}_2})] \dot{\alpha}$$

$$f_3 = \frac{M_{b_2} H_{b_1} H_{b_2}}{4} \dot{\theta}_{b_2}{}^2 \sin(\theta_{b_2} - \theta_{\mathrm{b}_1}) + [(\frac{M_{b_1} H_{b_1}{}^2}{4} + J_{b_1 xx} + M_{b_2} H_{b_1}{}^2 - J_{b_1 zz}) \sin\theta_{\mathrm{b}_1}$$
$$+ \frac{M_{b_2} H_{b_1} H_{b_2}}{4} \sin\theta_{\mathrm{b}_2}] \dot{\alpha}^2 \cos\theta_{b_1} + \frac{M_{b_1} + 2M_{b_2}}{2} g H_{b_1} \sin\theta_{b_1} - k(\theta_{b_1} - \theta_{b_2}) - c(\dot{\theta}_{b_2} - \dot{\theta}_{b_1}) \quad ,$$

$$f_4 = [(\frac{M_{b_2} H_{b_2}^{\ 2}}{4} + J_{b_2 xx} - J_{b_2 zz}) \sin\theta_{b_2} + \frac{M_{b_2} H_{b_1} H_{b_2}}{4} \sin\theta_{b_1}]\dot{\alpha}^2 \cos\theta_{b_2} + \frac{M_{b_2} g H_{b_2}}{2} \sin\theta_{b_2} - k(\theta_{b_2} - \theta_{b_1}) - c(\dot{\theta}_{b_2} - \dot{\theta}_{b_1}) - \frac{M_{b_2} H_{b_1} H_{b_2}}{4} \dot{\theta}_{b_1}^{\ 2} \sin(\theta_{b_2} - \theta_{b_1}) \quad (29)$$

$$\mathbf{SE}(\mathbf{q})\mathbf{u} = \begin{pmatrix} (1/R_w)(\tau_l + \tau_r) \\ (L_{b_1}/2R_w)\tau_l - (L_{b_1}/2R_w)\tau_r \\ -\tau_l - \tau_r \\ 0 \end{pmatrix}. \quad (30)$$